Available online at www.sciencedirect.com
SCIENCE DIRECT®
Carbohydrate Research 339 (2004) 1087–1092
Carbohydrate RESEARCH

Crystal structure of *N*-(benzyloxycarbonyl)aminoethyl-2,3,4,6-*tetra*-*O*-benzoyl-α-D-mannopyranoside: stabilization of the crystal lattice by a tandem network of N–H···O, C–H···O, and C–H···π interactions

O. Srinivas,[a] B. Muktha,[b] S. Radhika,[a] T. N. Guru Row[b,*] and N. Jayaraman[a,*]

[a]*Department of Organic Chemistry, Indian Institute of Science, Bangalore 560 012, India*
[b]*Solid State and Structural Chemistry Unit, Indian Institute of Science, Bangalore 560 012, India*

Received 15 January 2004; accepted 14 February 2004

Abstract—Single crystal X-ray analysis of an aminoethyl mannopyranoside, namely, *N*-(benzyloxycarbonyl)aminoethyl-2,3,4,6-*tetra*-*O*-benzoyl-α-D-mannopyranoside (**1**), shows that the compound crystallizes in the monoclinic space group $P2_1$, with two molecules in the unit cell. The mannopyranoside unit adopts a distorted $^4C_1$ conformation. An analysis of the intermolecular interactions reveals a tandem network of N–H···O, C–H···O, and C–H···π interactions responsible for stabilizing the crystal lattice.

Keywords: Carbohydrate; Crystal structure; Hydrogen bonding; Mannopyranoside; Weak interactions

1. Introduction

Solid-state organization of carbohydrates is governed generally by hydrogen-bonding interactions in well defined geometrical arrangements in the crystal lattice.[1] The presence of highly directional O–H···O hydrogen-bonding networks is an inbuilt feature of the hydroxyl groups abundant sugar pyranoses.[2,3] Although there are several crystal structure reports available on either partially or fully protected derivatives of pyranosides, the generality of noncovalent interactions responsible for the stability of crystalline lattice of the protected sugar derivatives remains to be understood in detail. The roles of weak interactions,[4] mainly arising from C–H···O and C–H···π interactions, are becoming increasingly important to understand the packing forces in the crystalline lattice of carbohydrates. From neutron diffraction structural analyses of several monosaccharides and cyclodextrins, Saenger and co-workers have performed a comparative analysis of O–H···O and C–H···O hydrogen bonding interactions in sugar structures.[5] It is fairly clear from these analyses that a complex array of noncovalent interactions, complementing each other, stabilizes the crystalline lattice of carbohydrates. We have reported recently that the persistent hydrogen bonding patterns of free sugars can be preserved in protected sugar derivatives also.[6] This observation was revealed from the single crystal X-ray structural analysis of 1,2,3,4,6-*tetra*-*O*-benzoyl-α-D-mannopyranose (mannose perbenzoate), the molecular packing of which is governed completely by relatively weaker C–H···π interactions. In our continuing efforts to understand the inherent noncovalent interactions in sugar derivatives, we have determined the single crystal X-ray structural analysis of a mannopyranoside, namely, *N*-(benzyloxycarbonyl)aminoethyl-2,3,4,6-*tetra*-*O*-benzoyl-α-D-mannopyranoside (**1**) and we have analyzed the crystal structure in detail to identify the noncovalent interactions responsible for the molecular packing in the crystal lattice. We observe an elaborate

* Corresponding authors. Tel.: +91-80-2293-2578/2403; fax: +91-80-2360-0529; e-mail: jayaraman@orgchem.iisc.ernet.in

0008-6215/$ - see front matter © 2004 Elsevier Ltd. All rights reserved.
doi:10.1016/j.carres.2004.02.009

network of N–H···O, C–H···O, and C–H···π interactions that stabilize the molecule in the solid state. The details of the structural analysis of **1** are presented herein.

2. Experimental

2.1. *N*-(Benzyloxycarbonyl)aminoethyl-2,3,4,6-*tetra*-*O*-benzoyl-α-D-mannopyranoside (1)

A solution of 2-*N*-benzyloxycarbonylamino ethanol (1.75 g, 9.0 mmol) in CH_2Cl_2 (20 mL) was added with $Hg(CN)_2$ (2.31 g, 9.1 mmol), $HgBr_2$ (1.64 g, 4.55 mmol), and powdered molecular sieves 4 Å, stirred for 20 min at room temperature and under N_2 atmosphere. A solution of 2,3,4,6-*tetra*-*O*-benzoyl-α-D-mannopyranosyl bromide (6.0 g, 9.1 mmol) in CH_2Cl_2 (15 mL) was added dropwise over a period of 10 min. The reaction mixture was stirred for 20 h, worked up and purified (SiO_2, hexane/EtOAc 3:2) to afford **1** (5.98 g, 86%) as colorless viscous syrup, which solidified upon storage over a period of time. Mp 114–116 °C. $[\alpha]_D$ −47.0 (*c* 2.0, $CHCl_3$). IR (KBr) *ν* 3369.0, 1731.7, 1703.8, 1601.6, 1523.5, 1452.1, 1267.9, 1126.2, 1109.8, 1069.3, 706.8. ^{1}H NMR (400 MHz, $CDCl_3$) *δ* 8.08 (dd, 2H, *J* = 7.1, 1.3 Hz, Ar), 8.04 (dd, 2H, *J* = 8.2, 1.3 Hz, Ar), 7.95 (d, 2H, *J* = 7.3 Hz, Ar), 7.83 (dd, 2H, *J* = 8.1, 1.3 Hz, Ar), 7.64–7.24 (band, 17H, Ar), 6.11 (app. t, 1H, *J* = 10.0 Hz, H-4), 5.90 (dd, 1H, *J* = 10.1 Hz, 3.2 Hz, H-3), 5.72 (dd, 1H, *J* = 3.1 Hz, 1.7 Hz, H-2), 5.38 (t, 1H, *J* = 5.4 Hz, NH), 5.17–5.11 (m, 3H, H-1, CH_2Ph), 4.67 (dd, 1H, *J* = 12.1 Hz, 2.5 Hz, H-6_a), 4.48 (dd, 1H, *J* = 12.1 Hz, 4.4 Hz, H-6_b), 4.43 (m, 1H, H-5), 3.94 (m, 1 H, CH_2CH_a-O), 3.68 (m, 1 H, CH_2CH_b-O), 3.52 (m, 2H, CH_2-N). ^{13}C NMR (100 MHz, $CDCl_3$) *δ* 166.2, 165.6, 165.5, 165.4, 156.5, 133.5–133.1, 129.8–128.1, 97.9, 70.3, 70.0, 69.1, 67.8, 66.9, 62.8, 40.8. ESI-MS: Calcd for $C_{44}H_{39}NO_{12}$: *m/z*: 796.2354 $[M+Na]^+$; found: 796.2341 $[M+Na]^+$. Anal. Calcd C 68.30, H 1.81, N 5.08; found: C 68.62, H 2.21, N 5.23.

2.2. Crystal structure analysis

Colorless and transparent crystals of **1** were obtained by slow evaporation of a saturated solution in Et_2O. A crystal of the size (0.16×0.25×0.06 mm) was checked for extinction under a polarizing microscope and then mounted on a Bruker AXS SMART APEX CCD diffractometer[7] with a crystal to detector distance of 6.03 cm. The data were reduced using SAINT PLUS[7] and the structure was solved by direct methods and refined using SHELXL[8] to $R = 0.033$. The hydrogen atoms were located by difference Fourier techniques and refined isotropically while all the nonhydrogen atoms were refined anisotropically.

3. Results and discussion

In our interest to synthesize photoswitchable carbohydrate clusters[9] incorporating α-mannopyranoside moieties, we have synthesized the amine tethered mannopyranoside, namely, *N*-(benzyloxycarbonyl)-aminoethyl-2,3,4,6-*tetra*-*O*-benzoyl-α-D-mannopyranoside **1** (Fig. 1).[10] Synthesis of **1** was carried out by the glycosylation of 2-*N*-benzyloxycarbonylamino ethanol with 2,3,4,6-*tetra*-*O*-benzoyl-α-D-mannopyranosyl bromide in the presence of $HgBr_2/Hg(CN)_2$ activators in CH_2Cl_2 to afford the desired glycoside **1** in 86% yield. Single crystals suitable for analysis were obtained upon slow evaporation of a solution of **1** in Et_2O. Compound **1** crystallized in the monoclinic space group $P2_1$ with $a = 10.409$ (6), $b = 10.007$ (6), $c = 19.463$ (2) Å, and $\beta = 99.416$ (10)° and two molecules constituted a unit cell ($Z = 2$) (Table 1). ORTEP of **1** is given in Figure 2, all significant bond distances, bond angles, and torsion angles are listed in Tables 2 and 3.

An analysis of the C–C bond lengths within the pyranose ring shows that the bond lengths are in the range between 1.501 and 1.520 Å. Amongst the bonds within the pyranose ring, exocyclic C1–O1 bond length of 1.393(3) Å is found to be the shortest. The bond lengths C5–O5 and O5–C1 are 1.432(3) and 1.413(3) Å, respectively. The shortening of C1–O1 bond compared to O5–C1 bond distance indicates a significant anomeric effect, as in the case of free sugar derivatives.[11] The bond lengths of the four benzoate groups are similar with a mean bond length of O–C 1.338 Å; *C* = *O* 1.195 Å; CO–C (aromatic) 1.479 Å, respectively. As in the case of mannose perbenzoate,[6] there is no unusual deviation for the pyranose ring angles and the angles ranged between

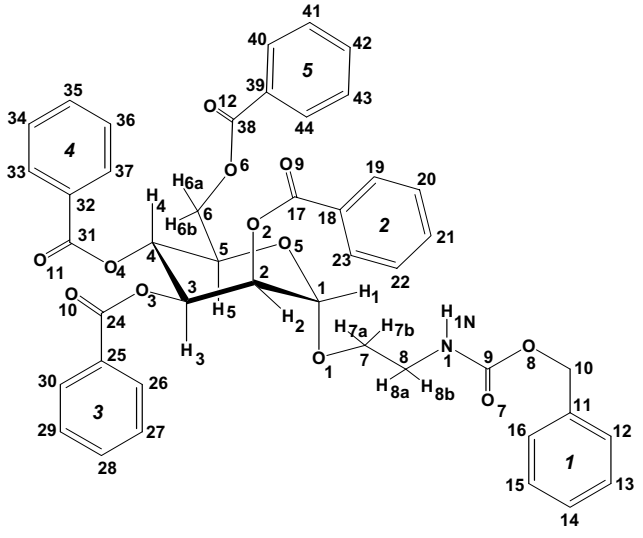

Figure 1. Molecular structure of **1**. Hydrogen atoms on the benzene rings are omitted for clarity. The number inside the aromatic rings denotes its position at a particular pyranose ring carbon atom.

Table 1. Experimental details

Crystal data	
Chemical formula	$C_{44}H_{39}NO_{12}$
Chemical formula weight (M_r)	773.79
Cell setting, space group	Monoclinic, $P2_1$
a, b, c (Å)	10.409 (6), 10.007 (6), 19.463(2)
β	99.416 (10)°
V (Å^3)	2000.3(2)
Z	2
D_x (Mg m^{-3})	1.28
Radiation type	Mo K$_\alpha$ radiation
No. of reflections for cell parameters	8302
θ range (°)	1.1–23.3°
Temperature (K)	293(2)
Crystal form, color	Block, white
Crystal size (mm)	0.16×0.25×0.06
Data collection	
Diffractometer	SMART APEX CCD area detector
Data collection method	ϕ scan
No. of measured, independent, and observed reflections	8302, 5316, and 4678
Criterion for observed reflections	$I > 2\sigma(I)$
R_{int}	0.013
θ_{max} (°)	23.3
Range of h, k, l	$-11 \rightarrow 11$, $-11 \rightarrow 8$, $-17 \rightarrow 21$
Absorption correction	SADABS
(T_{min}/T_{max})	0.9769/ 0.9944
Extinction correction	none
Refinement	
Refinement on	F^2
R, wR, S	0.033, 0.080, 1.083
No. of reflections and parameters used in refinement	5316 and 670
H-atom treatment	Isotropic
Weighting scheme	$w = 1/\sigma^2(F_0^2)$
$\Delta\rho_{max}$, $\Delta\rho_{min}$ (e Å^{-3})	0.172, −0.181

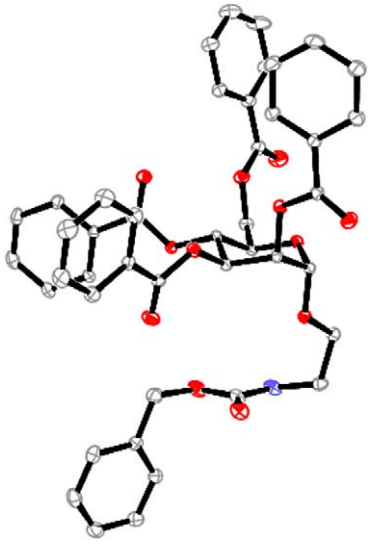

Figure 2. ORTEP of **1** with the displacement ellipsoids at 10% probability level.

Table 2. Selected bond lengths and bond angles (estimated standard deviations in parentheses)

Bond	Length (Å)	Bonds	Angle (°)
O5–C1	1.413 (3)	O5–C1–O1	112.86 (0.20)
C1–C2	1.508 (3)	O1–C1–C2	104.98 (0.20)
C2–C3	1.513 (3)	C2–C3–C4	109.69 (0.21)
C4–C3	1.502 (3)	C5–C4–C3	110.03 (0.22)
C5–C4	1.520 (3)	C1–C2–H2	110.36 (1.65)
O5–C5	1.432 (2)	O1–C7–C8	106.24 (0.22)
C1–H1	0.985 (23)	C1–C2–C3	109.15 (0.20)
O1–C1	1.393 (3)	O2–C2–C1	111.14 (0.21)
O1–C7	1.424 (3)	C1–O5–C5	113.97 (0.19)
C2–H2	0.954 (27)	O2–C17–O9	122.54 (0.24)
O2–C2	1.436 (3)	C2–C3–H3	112.62 (1.42)
O2–C17	1.346 (3)	O3–C3–H3	105.69 (1.53)
C3–H3	0.936 (25)	C3–O3–C24	118.09 (0.19)
O3–C3	1.436 (3)	O3–C3–C4	110.52 (0.21)
O3–C24	1.338 (3)	O4–C4–C3	109.17 (0.19)
O4–C4	1.441 (2)	O4–C31–O11	123.77 (0.24)
C4–H4	0.987 (22)	O4–C4–C5	107.47 (0.18)
O4–C31	1.339 (2)	C5–C4–C3	110.03 (0.22)
C5–C6	1.500 (4)	O5–C5–C6	107.34 (0.22)
O6–C6	1.437 (3)	O6–C6–H6A	108.20 (1.67)
O6–C38	1.330 (3)	O6–C6–H6B	107.03 (1.54)
O1–C7	1.424 (3)	C6–C5–H5	105.02 (1.31)
C7–C8	1.494 (4)	O6–C38–O12	123.37 (0.31)
N1–C8	1.449 (4)	C1–O1–C7	115.06 (0.19)
N1–C9	1.352 (4)	O1–C7–C8	106.24 (0.22)
O7–C9	1.202 (4)	O8–C9–O7	123.90 (0.31)
O8–C9	1.353 (3)	O8–C9–N1	109.89 (0.27)
O8–C10	1.447 (4)	O7–C9–N1	126.16 (0.33)

Table 3. Selected (torsion angles estimated standard deviations in parentheses)

Pyranose ring	Angle (°)
C5–O5–C1–O1	58.30 (0.26)
C5–O5–C1–C2	−59.49 (0.26)
C1–O5–C5–C6	−175.19 (0.21)
C1–O5–C5–C4	59.54 (0.25)
O5–C1–C2–O2	−60.80 (0.27)
O5–C1–C2–C3	55.54 (0.27)
O1–C1–C2–O2	176.75 (0.19)
O1–C1–C2–C3	−66.91 (0.25)
O5–C5–C4–O4	−176.57 (0.18)
O5–C5–C4–C3	−57.80 (0.25)
O5–C5–C6–O6	−75.36 (0.26)
C6–C5–C4–O4	63.01 (0.27)
C4–C5–C6–O6	45.71 (0.31)
O2–C2–C3–O3	−56.29 (0.25)
O2–C2–C3–C4	64.38 (0.25)
C1–C2–C3–O3	−175.97 (0.20)
C1–C2–C3–C4	−55.29 (0.27)
N-(benzyloxycarbonyl)aminoethyl segment	
C7–O1–C1–O5	62.31 (0.28)
C7–O1–C1–C2	−176.21 (0.21)
C1–O1–C7–C8	−174.22 (0.23)
C9–O8–C10–C11	−91.46 (0.37)
C9–N1–C8–C7	−96.96 (0.36)
C8–N1–C9–O8	167.10 (0.28)
C8–N1–C9–O7	−15.11 (0.53)
H(1N)–N1–C9–O8	0.56 (2.48)

Table 4. Hydrogen bond data for D–H···A bonds[a]

	D–H···A	D–H (Å)	H···A (Å)	D···A (Å)	D–H–A (°)
1.	N(1)–H(1N)···O(7)	0.884 (38)	2.239 (38)	3.011 (4)	145.79 (3.35)
2.	C(36)–H(36)··· O(5)	0.972 (36)	2.642 (35)	3.402 (4)	135.31 (2.54)
3.	C(8)–H(8A)··· O(10)	0.982 (31)	2.396 (33)	3.335 (4)	159.84 (2.63)

[a]Symmetry code: 1. $-x+1, +y-1/2, -z+1$; 2. $x+1$, +y,+z; 3. $-x+1, +y-1/2, -z+1$.

109.1° and 113.9°. It is observed further that the molecular features of **1** are found to be similar to those of (*R*)/(*S*)-3-benzyloxy-4-pentene-1-yl-2,3,4,6-*tetra*-*O*-benzoyl-α-D-mannopyranoside, reported by Ziegler et al.[12]

The valence bond angles of 113.9° and 112.8° in the sequence C5–O5–C1–O1, respectively, and the torsion angle 58.30 (0.26)° for the sequence C5–O5–C1–O1 indicate the α-configuration at the anomeric center. These values also correlate well to that found in the case of methyl-α-D-mannopyranoside.[11] The molecular conformation is a distorted $^4C_1$ with Cremer–Pople puckering parameters[13] $Q = 0.574$ Å, $\theta = 2.37°$, and $\varphi = 234.11°$. The torsion angles O5–C5–C6–O6 of −75.3° and C4–C5–C6–O6 of 45.7° indicate the *gauche–gauche* orientation of primary benzoyloxy group with respect to the ring oxygen as well as to the C-4 substituent. On the other hand, the torsion angles of C7–O1–C1–O5 of 62.3° and C7–O1–C1–C2 of −176.2° show that the anomeric substituent has *gauche–trans* orientation with respect to the pyranose ring. The benzoyl ester group conformation shows that the bond CO–COPh is nearly antiparallel and deviates from 180° by a value of 4.8° (C-2), 4.3° (C-3), 2.6° (C-4), and 3.2° (C-6). The torsion angle of the amino ethyl segment O1–C7–C8–N1 is 64.2°, indicating a *gauche* conformation for this anomeric substituent.

An analysis of the noncovalent interactions shows that an array of NH···O, C–H···O, and C–H···π interactions stabilizes the molecular packing in the crystal lattice of **1**. C–H···O hydrogen bond is a well-studied,[14] archetype of the classical hydrogen bond [15] such as OH···O and NH···O hydrogen bonds. It is characterized by the acidity of the C–H bond[16] and to an extent the basicity of the O-atom.[17] On the other hand, C–H···π interactions can be regarded as the weakest extreme of hydrogen bonds, which occurs between CH groups (soft acids) and π systems (soft bases).[18] The C–H···O bonds were identified based on the distance criterion of <2.7 Å and the angle constraint of C–H···O >120°. The C–H···π interactions were analyzed according to the approach formalized by Nishio and coworkers [19] and were identified using PARST97.[20] An intermolecular distance [D_{max} 3.05: 2.9 Å (for C–H) plus 1.7 Å (for a half thickness of the aromatic ring)×1.05] was considered relevant for the presence of C–H···π interaction.

Data on intermolecular interactions arising from NH···O and CH···O hydrogen bonds are presented in Table 4. When viewed along the *a* axis, each molecule in the crystal lattice interacts with another symmetry related molecule with the aid of these intermolecular hydrogen bonds. These two types of hydrogen bonds, specifically arising from N(1)–H(1N)···O(7) and C(8)–H(8a)···O(10) contacts, form a zig-zag chain, which runs down along the translation axis *b* (Fig. 3). The remaining C–H···O bond, arising from C(36)–H(36)···O(5), forms an infinite chain connecting molecules and is roughly perpendicular to the above two interactions. It is interesting to note that while the pyranose ring oxygen is known to behave as weak hydrogen-bond acceptor in free sugars[3] involving

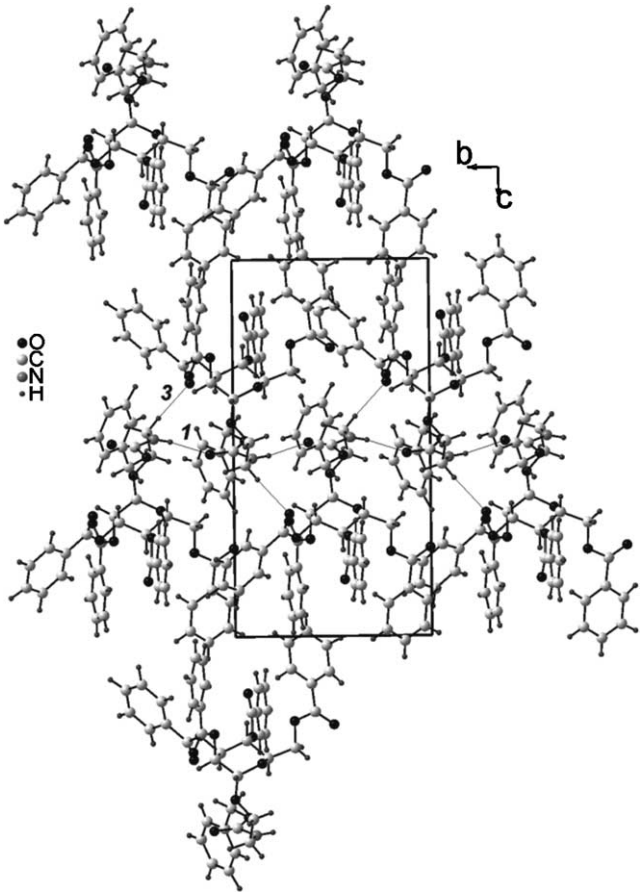

Figure 3. C–H···O and N–H···O interactions (packing along axis *a*). Numbers indicate the contacts as described in Table 4.

Table 5. Intermolecular C–H···π interactions[a]

	Interaction	D_{atm} (Å)	D_{lin} (Å)[b]	θ (°)	ω (°)	Label
1.	C35–H35···C39	2.881	2.879	39.16	113.01	4-H_{para}···5π
2.	C14–H14···C37	3.041	2.976	36.66	132.28	1-H_{para}···4π
3.	C28–H28···C33	2.851	2.942	33.79	110.13	3-H_{para}···4π
4.	C23–H23···C26	2.670	2.775	35.22	109.38	2-H_{ortho}···3π
5.	C7–H7A···C15	2.819	2.830	38.11	81.08	H7a···1π
6.	C36–H36···C14	3.010	3.134	49.01	111.96	4-H_{meta}···1π

[a]Symmetry code: 1. $x+1, +y, +z$; 2. $-x+2, +y+1/2, -z+1$; 3. $x, +y+1, +z$; 4. $x-1, +y, +z$; 5. $x-1, +y, +z$; 6. $-x+2, +y-1/2, -z+1$.
[b]D_{lin} is defined as the distance between the H-atom of the C–H moiety with the midpoint of the closest aromatic C–C bond, is closer to or shorter than D_{max}.

O–H···O hydrogen bonds, this property is fulfilled by an analogous C–H···O interaction in **1**. Amongst these three interactions, only the C(36)–H(36)···O(5) interaction involves the pyranose ring oxygen (O5) and also the *O*-benzoyl group at position 4 of the pyranose ring. The other two interactions are derived from *N*-(benzyloxycarbonyl)aminoethyl segment and contribute to the packing of the molecules along the translational axis *b*.

In addition to the above interactions, a network of C–H···π interactions that stabilize the packing motif is also observed. The geometric parameters of the C–H···π interactions are given in Table 5. There are six C–H···π contacts: the aromatic rings 1, 3, and 4 are observed to display both C–H···π donor and acceptor character, whereas aromatic rings 2 and 5 participate only as a donor and an acceptor, respectively. Within these, only aromatic ring 4 is found to act as a two-point donor. Another C–H···π interaction, arising from C7–H7a···C15, is also observed involving methylene proton of aminoethyl segment and the aromatic ring 1 of another molecule. This interaction, along with interaction arising from C36–H36···C14 contact, leads the aromatic ring 1 to behave as a two-point acceptor. The intermolecular C–H···π interactions when viewed along *a* axis are shown in Figure 4. The overall pattern of these interactions can be visualized as three inter-twinning networks. The first one is arising from 1-H_{para}···4π and 4-H_{meta}···1π contacts. This interaction is complementary to the N(1)–H(1N)···O(7) and C(8)–H(8a)··· O(10) hydrogen bonds and forms as an infinite chain running along the 2_1 screw axis. The second network of C–H···π connectivity arises from 4-H_{para}···5π,

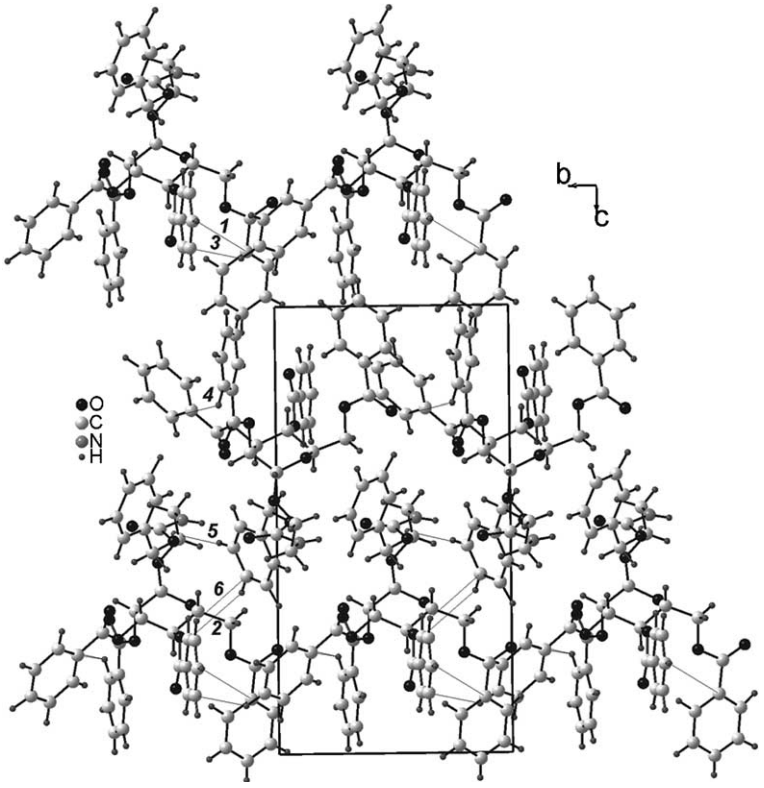

Figure 4. C–H···π interactions (packing along axis *a*). Numbers indicate the contacts as described in Table 5.

2-$H_{ortho}\cdots 3\pi$ and H7a$\cdots 1\pi$ and the third network originates from the 3-$H_{para}\cdots 4\pi$ interaction, in a direction perpendicular to both the first two networks.

4. Conclusions

The crystal structure analysis of the title compound is intriguing when compared to the mannose perbenzoate, whose crystal structure was reported earlier.[6] A comparison of these crystal structures shows that a single point alteration of the anomeric substituent of the pyranose can lead to drastic changes in the intermolecular contacts. We presume that the NH$\cdots$O hydrogen bond and subsequently the C–H$\cdots$O hydrogen bond play a major role in **1**. In addition to the role of stabilizing the molecular packing, the relatively much weaker C–H$\cdots\pi$ interactions in **1** also engage to preserve characteristic patterns of noncovalent interactions commonly found in sugar structures,[3] for example, the involvement of aromatic ring 1 as only a C–H$\cdots\pi$ acceptor, similar to one of the two C–H$\cdots$O interactions involving the pyranosidic oxygen. These observations consolidate the premonition that noncovalent interactions follow nearly a rigid pattern in both free and derivatized sugar structures in general. Such a pattern is fulfilled by involving a tandem network of NH$\cdots$O, C–H$\cdots$O, and CH$\cdots\pi$ interactions in the solid state structure of **1** analyzed herein.

5. Supplementary material

The crystallographic data were deposited at the Cambridge structural database (Accession number CCDC 224138). Copies of this information can be obtained free of charge from the Director, CCDC, 12 Union Road, Cambridge CB21EZ, UK (fax: +44-1223-336033; e-mail: deposit@ccdc.cam.ac.uk or http://www.ccdc.cam.ac.uk).

Acknowledgements

We thank the Department of Science and Technology, India for data collection on the CCD facility setup under the IRFA-DST program. NJ thanks Department of Science and Technology, India, for the financial support.

References

1. Jeffrey, G. A.; Saenger, T. *Hydrogen bonding in Biological Structures*; Springer: Berlin, 1991.
2. Ceccarelli, C.; Jeffrey, G. A.; Taylor, R. *J. Mol. Struct.* **1981**, *70*, 255–271.
3. Jeffrey, G. A.; Mitra, J. *Acta Cryst.* **1983**, *B39*, 469–480.
4. Desiraju, G. R.; Steiner, T. *The Weak Hydrogen Bond in Structural Chemistry and Biology*; Oxford University Press: Oxford, 1999.
5. (a) Steiner, T.; Saenger, W. *Acta Cryst. B* **1992**, *48*, 819; (b) Steiner, T.; Saenger, W. *J. Am. Chem. Soc.* **1992**, *114*, 10146.
6. Muktha, B.; Srinivas, O.; Amresh, M. R.; Guru Row, T. N.; Jayaraman, N.; Sekar, K. *Carbohydr. Res.* **2003**, *338*, 2005–2011.
7. Bruker SMART and SAINT. Bruker AXS Inc., Madison, Wisconsin, USA, **1998**.
8. Sheldrick, G.M. SHELXS97 and SHELXL97. University of Göttingen, Germany, **1997**.
9. Srinivas, O.; Mitra, N.; Jayaraman, N.; Surolia, A. *J. Am. Chem. Soc.* **2002**, *124*, 2124–2125.
10. Jayaraman, N.; Stoddart, J. F. *Tetrahedron Lett.* **1997**, *38*, 6767–6770.
11. Berman, H. M.; Chu, S. S. C.; Jeffery, G. A. *Science* **1967**, *157*, 1576–1577.
12. (a) Ziegler, T.; Bien, F.; Frey, W. *Z. Kristallogr. NCS* **1998**, *213*, 611–612; (b) Ziegler, T.; Bien, F.; Frey, W. *Z. Kristallogr. NCS* **1998**, *213*, 613–614.
13. Cremer, D.; Pople, J. A. *J. Am. Chem. Soc.* **1975**, *97*, 1354–1358.
14. Desiraju, G. R. *Acc. Chem. Res.* **1996**, *29*, 441–449.
15. Jeffrey, G. A. *J. Mol. Struc.* **1999**, *485–486*, 293–298.
16. Desiraju, G. R. *J. Chem. Soc., Chem. Commun*. **1989**, 179–180.
17. Steiner, T. *J. Chem. Soc., Chem. Commun.* **1994**, 2341–2342.
18. Nishio, M.; Hirota, M.; Umezawa, Y. *The CH/π Interaction: Evidence, Nature and Consequences*; Wiley-VCH: New York, 1998.
19. Takahashi, H.; Tsuboyama, S.; Umezawa, Y.; Honda, K.; Nishio, M. *Tetrahedron* **2000**, *56*, 6185–6191.
20. Nardelli, L. J. *Appl. Crystallogr.* **1995**, *28*, 659.